J. CHEM. SOC. FARADAY TRANS., 1993, 89(7), 1007–1019

Photosensitizers: Comprehensive Photophysics/Photochemistry and Theory of Coumarins, Chromones, their Homologues and Thione Analogues

Ralph S. Becker,* Sankar Chakravorti and Carlos A. Gartner
Department of Chemistry, University of Houston, Houston, TX 77204-5641, USA
Maria de Graca Miguel
Departmento de Quimica, Universidade de Coimbra, Coimbra, Portugal

The photophysical–photochemical behaviour, including absorption spectra, fluorescence spectra and lifetimes, phosphorescence spectra, triplet–triplet transient spectra, triplet lifetimes and quantum yields and sensitized singlet oxygen formation and yields, has been determined for many of a group of 22 carbonyl and thione compounds. These include coumarins, psoralens, chromones and furochromone and their thiones. Many of the thiones were synthesized for the first time. Two types of theoretical calculations were carried out on the majority of the compounds. The principal goals of the research for the thiones, were (1) to produce or improve the photosensitizer capabilty of the compounds *in vivo*, (2) to shift the spectra of the compounds to significantly longer wavelength and (3) to increase the triplet and singlet oxygen quantum yields. Most of these have been largely achieved. The photosensitizing abilities of two of the thiones have been evaluated using a unique testing technique employing a series of genetically engineered bacteria.

Typically, the coumarins, chromones and their homologues of interest, the furanocoumarins (psoralens) and furochromones absorb largely in the UV-B and UV-C, although there can be some absorption in the UV-A for some furo homologues. Also, many if not most of these commonly have relatively low triplet yields; moreover, the quantum yields for energy transfer to form singlet oxygen are still lower by 50–60%. In general we wished to evaluate, or re-evaluate in several cases, the photophysical properties of the foregoing photosensitizers and importantly, to determine how these were altered when going to the corresponding thione compound.

Although there are some photophysical and chemical data on psoralen[1–3] there are none on the thione derivatives, nor are there any calculations, or singlet oxygen yield data on the latter. Even then, there is some confusion about the triplet quantum yield (ϕ_T) of some psoralens. There are no triplet data on the coumarins and thione chromone of concern here, and there are limited data on the thione coumarins and little or no calculations. Finally, for the two photosensitizers khellin and visnagin and their thione analogues, no triplet data, little or no fluorescence data and few or no calculations exist. There is considerable information regarding S_2 emission, room-temperature phosphorescence, self-quenching and there is some information on triplet energy transfer to form singlet oxygen for a variety of general thiones.[4–12]

Typically, several psoralens[1,2,13,14] khellin and visnagin have been found to be photoactive against cells and viruses for example.[15] However, they typically absorb on the short-wavelength edge of the UV-A region where many other biomolecules also absorb.

Based on all of the foregoing, our more specific goals were: (1) to shift the absorption spectrum of a wide variety of molecules as far as the visible region, (2) to be able to predict *via* theoretical calculations the absorption spectral properties of the molecules of concern, orbital origins, charge densities and the like, (3) to increase the triplet quantum yield, (4) to increase the quantum yield of $^1O_2$ formation and (5) to create new active effective *in vivo* photosensitizers. Furthermore, in a cooperative testing program, the biological evaluation of the photosensitizing dynamics of two new thione compounds has been completed utilizing genetically engineered *E. coli* bacteria.[14–17] Thus, not only does this work offer a broad-based examination of photophysical, photochemical, theoretical and sensitizer aspects, but provides some new insight into the mechanisms and targets of *in vivo* activity.

The photophysical–photochemical data at room temperature include absorption spectra, triplet–triplet (T–T) spectra, triplet kinetics, triplet quantum yields, fluorescence spectra, fluorescence kinetics, phosphorescence spectra and sensitized singlet oxygen formation and yields. In addition, theoretical calculations of the semiempirical type employing π-electrons only (MO-SCF-CI-PPP) and π and σ electrons (INDO/S-CI) were carried out on a large number of molecules.

Experimental

The compounds studied are shown in Fig. 1 along with their trivial and systematic names.

All solvents were spectroscopic grade and were used without further purification. Absorption spectra were obtained on one of several instruments including a Hewlett Packard Model 8450 and a Cary model 15.

The laser flash experimental set-up has been described previously.[18] A Q-switched Nd : YAG laser with an 11 ns pulse width was employed. The wavelength commonly employed was 355 nm, although in some cases (such as chromone), 266 nm was necessary. The intensity of the laser radiation was controlled by a polarizer attenuator (Glan-laser polarizing prisms). The solutions were examined in a rectangular quartz cell of 10 mm pathlength along the monitoring light path and saturated with argon, nitrogen or oxygen.

Fluorescence and phosphorescence were obtained on a Spex Industries Datamate automatic scanning and acquisition system with model 1681 exciting and analysing monochromators (1200 grooves cm^{-1}, effective *f*4) and a cooled (−10 °C) housing containing an IP21 photomultiplier tube. The reciprocal dispersion was 3.7 nm mm^{-1}, resolution was 0.25 nm at 546 nm with a 50 μm slit and the operating range was 200–1000 nm.

The precision for wavelengths of maxima of triplet–triplet absorption are ±5–10 nm, for UV–VIS absorption ±2–3 nm, and for fluorescence and phosphorescence, ±2–5 nm.

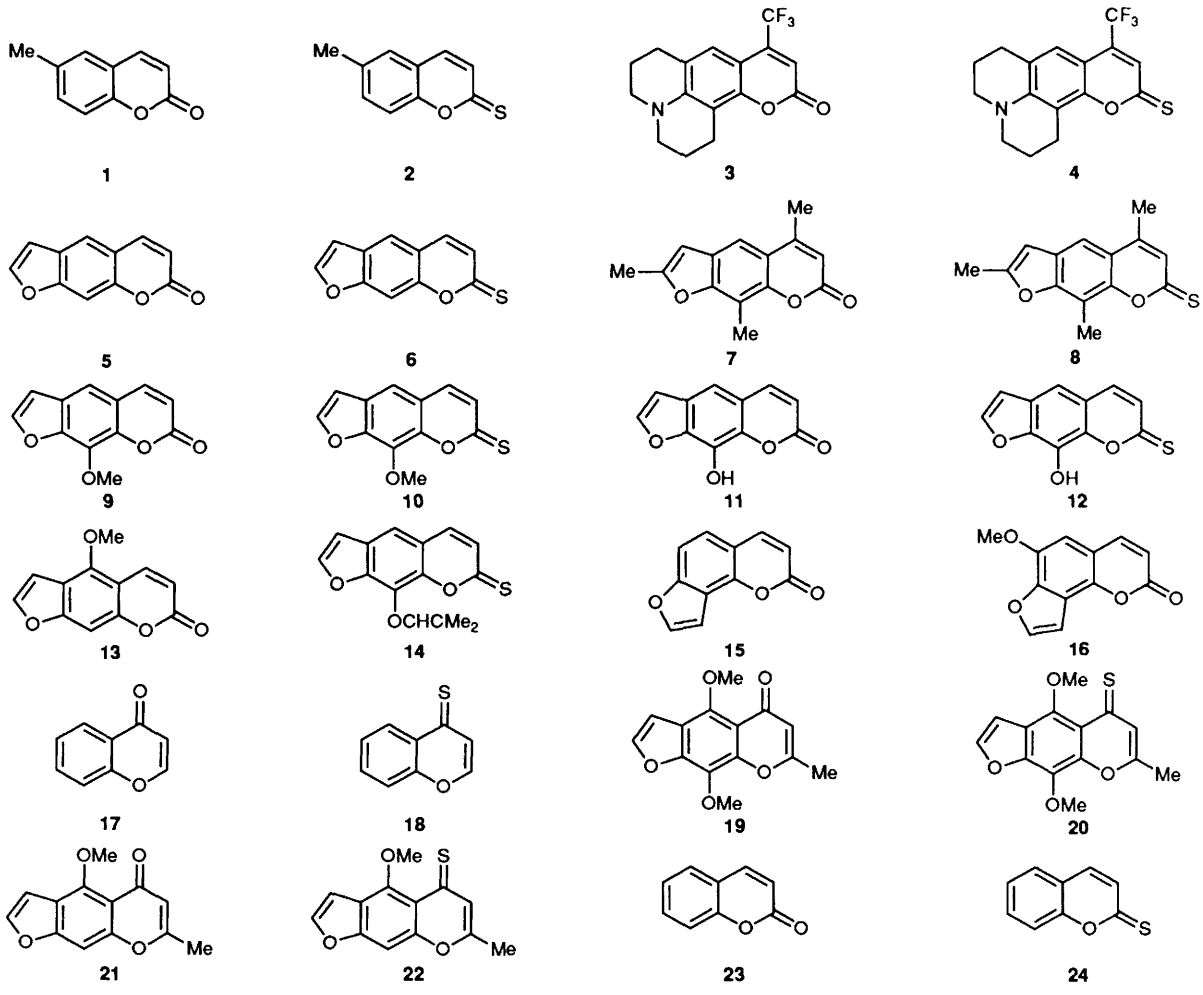

compound no.	trivial name	systematic name
1	6-methyl coumarin	6-methyl-1-benzopyran-2-one
2	6-methyl thione coumarin	6-methyl-1-benzopyran-2-thione
3	coumarin 153	9-trifluoromethyl-2,3,6,7-tetrahydro-1*H*,5*H*-[1]benzopyrano[6,7,8-*ij*]quinolizin-11-one
4	thione coumarin 153	9-trifluoromethyl-2,3,6,7-tetrahydro-1*H*,5*H*-[1]benzopyrano[6,7,8-*ij*]quinolizine-11-thione
5	psoralen	furo[3,2-*g*][1]benzopyran-7-one
6	thione psoralen	furo[3,2-*g*][1]benzopyran-7-thione
7	4,5′,8-trimethyl psoralen	2,5,9-trimethylfuro[3,2-*g*][1]benzopyran-7-one
8	4,5′,8-trimethyl thione psoralen	2,5,9-trimethylfuro[3,2-*g*][1]benzopyran-7-thione
9	8-methoxypsoralen	9-methoxyfuro[3,2-*g*][1]benzopyran-7-one
10	8-methoxy thione psoralen	9-methoxyfuro[3,2-*g*][1]benzopyran-7-thione
11	8-hydroxypsoralen	9-hydroxyfuro[3,2-*g*][1]benzopyran-7-one
12	8-hydroxy thione psoralen	9-hydroxyfuran[3,2-*g*][1]benzopyran-7-thione
13	5-methoxypsoralen	4-methoxyfuro[3,2-*g*][1]benzopyran-7-one
14	imperatorin	8-isobutoxyfuro[3,2-*g*][1]benzopyran-7-one
15	angelicin	furo[3,2-*h*]-1-benzopyran-2-one
16	sphondin	6-methoxyfuro[3,2-*h*]-1-benzopyran-2-one
17	chromone	1-benzopyran-4-one
18	thione chromone	1-benzopyran-4-thione
19	khellin	4,9-dimethoxy-7-methylfuro[3,2-*g*][1]benzopyran-5-one
20	thione khellin	4,9-dimethoxy-7-methylfuro[3,2-*g*][1]benzopyran-5-thione
21	visnagin	4-methoxy-7-methylfuro[3,2-*g*][1]benzopyran-5-thione
22	thione visnagin	4-methoxy-7-methylfuro[3,2-*g*][1]benzopyran-5-thione
23	coumarin	1-benzopyran-2-one
24	thione coumarin	1-benzopyran-2-thione

Fig. 1 Structures of compounds studied

None of the emission spectra are corrected for photomultiplier tube response; generally, in the region of 500 nm, maxima would be red shifted by *ca.* 20 nm.

Fluorescence lifetimes were obtained on a model 1712 Photochemical Research Association photon-counting fluorescence lifetime instrument with a Tracor Northern multichannel analyser and a Hewlett Packard 7225B graphics plotter, or a photon-counting instrument system using a mode-locked, synchronously pumped cavity-dumped dye laser (Nd : Yag. Laser). The systems contained deconvolution software and statistical analyses to perform reduced χ^2, runs, and Durbin–Watson tests as well as determine weighted residuals.[19,20] All of the foregoing tests were employed to obtain the most reliable decay lifetimes.

In general, for T–T spectra, laser input energies were from 3–8 mJ per pulse at 355 nm. On the other hand for lifetimes and quantum yields (see below), energies were kept as low as possible to minimize or avoid non-linear effects and triplet–triplet quenching. Commonly, these energies were in the range $\leqslant$1–3 mJ per pulse at 355 and 266 nm (in some cases up to 5 mJ for lifetime). Identification of transients as triplets was commonly performed by observing the rise of the, β-carotene triplet by energy transfer. In some cases of homologues or analogues, observation of oxygen quenching was used instead. The initial absorbances (A) were kept low, generally 0.1–0.3 per 10 mm path at 355 nm (or 266 nm) (concentrations 10^{-5}–10^{-4} mol dm^{-3}).

In general, triplet quantum yields are $\pm$15% and triplet lifetimes are $\pm$10–15% (with some exceptions that will be noted). Triplet quantum yields were determined either by the partial depletion technique or by the technique of energy transfer to β-carotene.[21]

For the energy-transfer technique, optically matched solutions (*ca.* 2 cm^3, $A \approx 0.2$ in 1 cm cell) benzophenone (actinometer) and the unknowns in benzene at 355 nm were mixed with a known volume (0.1–0.2 cm^3) of a 1.0 mmol dm^{-3} solution of β-carotene in benzene. The transient absorbance (ΔA) of β-carotene at 540 nm, formed by energy transfer from the samples (unknown or benzophenone), was monitored. With the help of the following expression (see also ref. 21 and 22), ϕ_T was estimated

$$\phi = \phi^a \frac{\Delta A^u}{\Delta A^a} \frac{-(k^u_{obs})(k^a_{obs} - k^a_0)}{(k^a_{obs})(k^u_{obs} - k^u_0)}$$

where ϕ_T, ΔA, k_{obs} and k_0 are the triplet yield, the plateau absorbance following the completion of sensitized triplet formation, the pseudo-first-order rate constant for the growth of the β-carotene triplet sensitized by a unknown or benzophenone and the rate constant for the decay of the donor triplet, respectively. Here, the first-order decay rate constant of the β-carotene triplet is considered to be much less than k_{obs} which is determined experimentally. The superscripts u and a refer to the type of sample (unknown and benzophenone actinometer, respectively). At the laser energies used, β-carotene solution alone shows no formation of a triplet transient on excitation. The ϕ_T data obtained by this method are reliable to the extent that the assumption of 100% energy transfer to β-carotene is valid.

For the depletion technique, the ε_T for the unknown was obtained from the following equation:

$$\varepsilon_T(\lambda_1) = \varepsilon_{GS}(\lambda_2) \frac{\Delta A_T(\lambda_1)}{\Delta A_S(\lambda_2)}$$

where $\varepsilon_T(\lambda_1)$ is the absorption coefficient for the triplet at λ_1, $\varepsilon_{GS}(\lambda_2)$ is the absorption coefficient for the $S_0 \rightarrow S_n$ absorption at λ_2, $\Delta A_T(\lambda_1)$ is the intensity of absorption at λ_1 and ΔA_S is the intensity of the depletion at λ_2. The absorbances were determined as the slope of a plot of ΔA *vs.* laser energy per pulse measured as per cent transmission of a polarizer attenuator (three or four different values of per cent transmission were used). The assumption was made that the triplet–triplet absorption was negligible at the wavelength at which the singlet depletion was monitored (near the maximum of the first singlet transition). The ε_T values obtained by this assumption will be upper limits for the actual ε_Ts. ϕ_T values were then determined by the comparative method[21] using benzophenone in benzene as the reference actinometer ($\varepsilon = 7220$ dm^3 mol^{-1} cm^{-1}, $\phi_T = 1$). The solution of the actinometer and unknown were optically matched at 355 nm.

Singlet oxygen quantum yields (ϕ_Δ) were measured by one or two techniques. One method used steady-state excitation using the 1,3-diphenylisobenzofuran (DPBF) bleaching technique.[23] The other method involved the infrared emission technique using pulsed excitation.[24] The luminescence signal intensity at 1.27 μm was measured by extrapolating the long-lived exponential component due to singlet oxygen alone to zero time to eliminate any errors arising from sample fluorescence or phosphorescence and light scattering (if any). The linearity with respect to three different input laser energies was checked. Each time the 1.27 μm signal was averaged from 20 shots. In both techniques, the original solutions were saturated with O_2 (and repeated if necessary). ϕ_Δ has an error of $\pm$15–20%.

Calculations of the intermediate neglect of differential overlap type (INDO) were performed with the INDO/S-CI model.[25] The configuration interaction (CI) consisted of 196 selected single excited configurations. The two-centre electron repulsion integrals for both INDO/S and PPP were estimated using the Mataga–Nishimoto approximation. Calculations in the π-electron-only approximation followed that of Pariser, Parr and Pople (PPP)[26] with a singly excited CI calculation. Parameters used in PPP calculations of the various molecules are shown in Table 1, where h and k are the usual Hückel parameters; E_i is the ionization potential, γ is the one-centre repulsion integral and β_{SCF} is the core integral. Molecular coordinates were commonly obtained from minimum-energy geometries determined by a PC model molecular modelling software program (Serena Sofware, Bloomington, IN) employing an MMX force field including π-system routines.

Synthesis of various compounds was accomplished as follows. After we had initiated the synthesis and study of the thionepsoralens, we found a reference to the synthesis of two of them and their activity towards a yeast.[27]

In general, the proton NMR of the thione products were very similar to their ketone parent counterparts except that particularly the proton on the adjacent carbon (H_a) to the thione was shifted to a lower field but the coupling constant to H_b stayed constant. Therefore a detailed NMR will be given only for **1** and **2** as representative of the coumarins and furanocoumarins (psoralens); moreover, a detailed NMR will be given for **19** and **20** as representative of chromone and furanochromones and their thiones.

1 (1.09 g) was combined with Lawesson's reagent (2.78 g) and toluene (100 cm^3) and the flask fitted with a reflux condenser and calcium chloride drying tube. The mixture was stirred at 92 °C for 30 min and all material dissolved. When a TLC with benzene–dichloromethane (1 : 1) showed predominantly starting material, Lawesson's reagent (254 mg) was added and the solution stirred for 30 min more. At this point, a TLC still showed some starting material, as well as product ($R_f = 0.63$), and Lawesson's reagent (254 mg) was again added. The mixture was stirred another 30 min, but not all material dissolved. A TLC showed little starting material at

Table 1 Parameters for PPP calculations

	h				k^a				E_i/eV				γ				$\beta_{SCF}{}^a$			
	C	O[b]	O[c]	S[c]	C—C	C—O	C=O	C=S	C	O[b]	O[c]	S[c]	C	O[b]	O[c]	S[c]	C—C	C—O	C=O	C=S
5	0.0	2.0	1.2	—	1.0	0.8	1.0	—	11.40	32.90	17.70	—	10.80	21.50	15.20	—	−2.4	−2.4	−2.4	—
15	0.0	2.0	1.2	—	1.0	0.8	1.0	—	11.20	32.90[d]	17.70	—	11.10	17.70	15.20	—	−2.4	−2.4	−2.4	—
16	0.0	2.0	1.2	—	1.0	0.8	1.0	—	11.20	32.90	17.70	—	11.10	2150[d]	15.20	—	−2.4	−2.4	−2.4	—
6	0.0	2.0	—	0.9	1.0	0.6	—	1.2	11.20	32.90	—	12.90	11.10	21.50	—	9.90	−2.2	−2.2	—	−2.0
1	0.0	2.0	1.2	—	1.0	0.8	1.0	—	12.20	32.90	17.70	—	11.60	21.50	15.20	—	−2.4	−2.4	−2.4	—
2	0.0	2.0	—	0.9	1.0	0.6	—	1.2	12.20	32.90	—	12.90	11.10	21.50	—	9.90	−2.2	−2.2	−2.4	−2.0
17	0.0	2.0	1.2	—	1.0	0.8	1.0	—	11.20	26.70	17.70	—	11.10	15.70	15.20	—	−2.4	−2.4	−2.4	—
18	0.0	2.0	—	0.9	1.0	0.6	—	1.2	11.20	26.70	—	12.90	11.10	15.70	—	9.90	−2.2[e]	−2.2[e]	—	−1.8
21	0.0	2.0	0.0	—	1.0	0.8[f]	1.0	—	11.20	26.70	17.70	—	11.10	15.70	15.20	—	−2.4	−2.4	−2.4	—
19	0.0	2.0	1.2	—	1.0	0.6[f]	1.4	—	11.20	30.80	17.70	—	11.10	17.50	15.20	—	−2.4	−1.9	−2.4	—

[a] C—C and C—O indicate the carbon–carbon and carbon–oxygen bonds normally in the ring except additional ones for C—O of C—OCH_3 in **21** and **19**. [b] Two electrons donated to the π system. [c] One electron donated to the π system. [d] For O of OCH_3, actually considered as OH, $E_i = 27.20$ eV and γ is 14.60. [e] The O(1)—C(2), C(2)—C(3) and C(3)—C(4) of the heterocyclic ring had values of −2.0 for β. [f] For CO of $COCH_3$, actually considered as COH, value is 1.1.

this time. However, a side product was present in large amounts. The solvent was removed by evaporation and the remaining solid dissolved in dichloromethane. White insoluble material was filtered off and discarded. The rest of the solution was run through a silica gel column using benzene as the eluent. The solvent was removed by evaporation and pure **2** (253 mg) was then crystallized from hexane (23% yield), m.p. 159–161 C. This low yield was attributed to formation of large amounts of a side product, incomplete reaction of the starting material and difficulties in purification.

The same reaction was run using phosphorus pentasulfide in toluene. The reaction was allowed to run overnight at 85 °C, the toluene removed by evaporation and the product was passed through a silica gel column using benzene as the eluent. The solvent was removed by evaporation and pure **2** crystallized from hexane in 59% yield.

For **1**, the methyl protons were at 2.410 ppm, the proton adjacent (a) to the ketone occurred as a doublet at 6.392 and 6.424 ppm, the proton at position b to the ketone showed up as a doublet at 7.647 and 7.679 ppm, and a multiplet occurred in the region 7.219–7.366 ppm. For **2**, the methyl proton peaks were almost unchanged in location (2.422 ppm), the H_a proton was shifted downfield (7.195 and 7.235 ppm), the H_b proton was slightly shifted upfield into the multiplet. The coupling constant remained essentially unchanged at 5.30 Hz. The multiplet covered the region 7.195–7.422 ppm.

9 (500 mg) was combined with Lawesson's reagent (1.12 g) and toluene (65 cm^3). The solution was heated to 74 °C and stirred for 4 h. All material dissolved at elevated temperatures. When a TLC with benzene–dichloromethane (1 : 1) showed starting material and a side product, more Lawesson's reagent (95 mg) was added and the solution was stirred for a further 1 h. At this point, a TLC showed an increasing amount of side product, the desired product (R_f = 0.50) and no further depletion of starting material. The solution was then allowed to cool to room temperature and a white material precipitated, was filtered off, and discarded. Toluene was then removed by evaporation and the product was eluted from a silica gel column with 5% methanol in benzene. Pure **10**, 102 mg, was crystallized from a benzene–ethanol mixture (21% yield), m.p. 198 °C. Our reported m.p. and ^1H NMR spectrum agree with those reported by others[27] (m.p. 198–199 °C). Our low yield was attributed to incomplete reaction and formation of large amounts of side product and P_2S_5 is recommended. When P_2S_5 was used the yield increased to 62%.

7 reacted with Lawesson's reagent to give only a 20% final yield of **8**. When P_2S_5 was used, a 60% yield was obtained. **7** (100 mg) was combined with P_2S_5 (292 mg) in pre-dried benzene and the mixture was heated at 70 °C. At this point 4–5 drops of piperidine were added and the mixture was stirred for 12 h. TLC analysis using benzene showed essentially complete reaction, $R_f = 0.57$ for **8**. Benzene was removed by evaporation and the product was eluted from a silica gel column with benzene. The solvent was removed by evaporation and the product was recrystallized from dichloromethane–2-methylbutane. **8** had an m.p. of 246–248 °C.

6, m.p. 181 °C, was synthesized in a similar manner to **10** and **8**. Our reported m.p. and ^1H NMR spectrum agree with those reported by others[27] (m.p. 180–181 °C). It is often difficult to remove all of the Lawesson's reagent and so use of P_2S_5 is recommended for coumarins and psoralens in general.

For **17**, sodium hydride (5 g) was suspended in anhydrous diethyl ether (80 cm^3) in a throughly dried flask and ethyl formate (33.5 g) was added with stirring (the flask was fitted with a dry reflux condenser). The entire system was kept under nitrogen. At this point 2-hydroxyacetophenone (7 g) was gradually added to the flask using ice to cool the vigorous reaction when necessary. When all reactants had been combined and the reaction had apparently subsided, the mixture was brought to reflux for 10 min and then stirred at room temperature overnight. Ice (200 g) and water were then very carefully added and two extractions were performed with ether. The aqueous layer was then freed from ether under vacuum and acidified with glacial acetic acid. The mixture was cooled with ice and a slurry of white material precipitated. This material (2-hydroxy-ω-formylacetophenone) was filtered and placed in a round-bottomed flask with a reflux condenser and sulfuric acid solution (16 cm^3 96% sulfuric acid, 70 cm^3 water) was added. The solution was heated to 89 °C for 20 min. It was then allowed to cool to room temperature and was neutralized with sodium hydrogencarbonate. **17** precipitated and was allowed to stand before being filtered off and dried. The product was recrystallized from petroleum ether and colourless crystals were collected in 77% yield. A melting point of 54 °C was found for the crystals, which is slightly below that reported in the literature.[28]

17 (518 mg) was mixed with Lawesson's reagent (1.15 g) in a round-bottomed flask and benzene (30 cm^3) was added. The solution was refluxed for 15 min at which point a TLC (dichloromethane mobile phase) showed virtually no starting material and essentially no side reactions. The solvent was then evaporated and the remaining material was purified

twice through a silica gel column using dichloromethane. **18** was then crystallized from petroleum ether as cherry-red crystals of melting point 85–87 °C (85% yield).

19 (300 mg) was combined with Lawesson's reagent (560 mg) in benzene. The mixture was stirred and refluxed for 30 min and the reaction monitored by TLC (2% methanol in chloroform). At this point, the benzene was removed by evaporation to give a dark red compound which was eluted from a silica gel column using 10% acetonitrile in benzene as the mobile phase. The product was crystallized from dichloromethane–ether to yield deep purple crystals. A TLC showed traces of impurities and the product was used without further purification (m.p. 148 °C). **22** was prepared in a similar fashion. In the case of **19**, the H_a proton (on the carbon adjacent to the ketogroup) occurred at 6.07 ppm, the protons of the adjacent methyl at 2.04 ppm, the protons of the methoxy at 4.06 and 4.20 ppm, and the protons of the furan ring were present as doublets in the 7.02 and 7.64 ppm region. For **20** the H_a proton shifted downfield into the doublet near 7.02 ppm while the remaining protons barely shifted at all (*ca.* 0.1 ppm downfield). The coupling between the furan ring protons did not change (2.1 Hz).

Results

In the Experimental section, we described the conditions for obtaining data and the errors expected. In addition in one case, **6**, we examined the effect of concentration on the triplet lifetime at a low energy input of 1–2 mJ per pulse. The concentrations were 30×10^{-6}, 16×10^{-6} and 8×10^{-6} mol dm^{-3} with absorbances of 0.37, 0.21 and 0.1, respectively, at 355 nm. The linear plot extrapolated to zero concentration gave a lifetime of 1.6 μs compared to 1.1, 1.3 and 1.4 μs for the foregoing absorbance/concentration combinations, respectively. It is clear that there can be considerable self-quenching at sufficiently high concentration, as has been established by others.[4,5] We believe that in the concentration range we used (*ca.* 10^{-5}–10^{-4} mol dm^{-3}, $A = 0.1$–0.3), in general the triplet lifetimes do not represent intrinsic ones.

Table 7 (later) provides data comparing theory and experiment regarding transition energies and intensities.

Discussion

One of the major goals was to increase the triplet yield (ϕ_T) and this could in turn increase the yield of singlet oxygen (ϕ_Δ). One of the ways to do this is to have the lowest excited singlet state of n, π^* character (*cf.* π, π^*).[29] The presence of a thione *vs.* ketone moiety can lead to such a result primarily because of the significant lowering of the ionization energy of the non-bonding (n) electrons of sulfur compared to oxygen.[29] We found that this was the case and both ϕ_T and ϕ_Δ were strongly enhanced in many instances (*vide infra*).

From the point of view of the photophysical aspects of phototoxin design, high triplet yields and/or high singlet oxygen yields are highly desirable. Also, of course, absorption in the visible region is of importance so that other biomolecules are not damaged (also low-energy spectral lamp sources can be used in place of UV). Other more biological aspects are obviously important such as the water or lipid solubility of the compounds.

We begin with consideration of the psoralens and thione psoralens since certain photophysical properties such as room-temperature phosphorescence are best seen and authenticated here. Since psoralens are an 'old' topic and data exist for comparison and discussion, these will be considered first.

Psoralens and Thione Psoralens

Compounds **5**–**11** and **13**–**16** were investigated (Table 2). The ϕ_T values were measured in methanol by the partial depletion technique.

Table 3 provides data comparing theory, using INDO/S and PPP, and experiment relative to transition energies/wavelengths, intensities and orbital origin assignments.

Theoretical Calculations of State Energy Order : Psoralens

For the carbonyl psoralens, theory, both INDO and PPP, predicts four $\pi \rightarrow \pi^*$ electronic transitions between *ca.* 350 and *ca.* 250 nm for psoralens (Table 3). In addition to the $\pi \rightarrow \pi^*$ transitions, $n \rightarrow \pi^*$ transitions are predicted at *ca.* 360 nm. Note how very close these are to the lowest $\pi \rightarrow \pi^*$ transitions (Table 3). It is impossible to know from the calculation whether an n, π^* or π, π^* singlet state is lowest. We believe that unless the n, π^* is predicted to be $\geqslant 2000$ cm^{-1} below the lowest $\pi \rightarrow \pi^*$ state, it is not possible to predict that the nature of the lowest excited singlet state is in fact n, π^*. The PPP predictions are in general in better agreement with experiment for psoralen than the INDO predictions.

For the isopsoralen **15**, INDO predicts the $\pi \rightarrow \pi^*$ transitions at somewhat longer wavelengths than found, while the agreement with PPP is very good (Table 3). Both INDO and PPP predict a small blue shift of the first $\pi \rightarrow \pi^*$ transition compared to **5**, as is observed (Table 3). In general, there is considerable similarity in the transitions of **15** and **5** both theoretically and experimentally but the separation of the first two $\pi \rightarrow \pi^*$ transitions is clearly greater for **5** (Table 3).

In general, the overall spectral appearance of **16** is very similar to **5** and **9** (except for the first weaker transition in **9**). From INDO calculations the location of the $\pi \rightarrow \pi^*$ transitions is in excellent agreement with experiment, definitely better than for the parent **15**. PPP calculations are also in very good agreement with experiment (as for **15**). For both **15** and **16**, $n \rightarrow \pi^*$ transitions are predicted to be of lowest energy (Table 2). Again they are predicted to be very close to the lowest $\pi \rightarrow \pi^*$ transitions. For **16**, the first $n \rightarrow \pi^*$ and $\pi \rightarrow \pi^*$ are predicted to be degenerate (Table 3).

Others[30,31] have examined the spectra of some psoralens (**5**, **7**, **9** and **15**). In general, there is agreement for the first absorption band and for those other bands where the compounds were studied in more detail (**5** and **9**). PPP calculations were also performed on two of the molecules of concern here: **5** and **9**. In general, the wavelengths were in good agreement with experiment but the oscillator strengths were not as well predicted as ours for at least the first two transitions.

We could not observe any $n \rightarrow \pi^*$ transitions experimentally.

Photophysical : Psoralens

There has been some considerable confusion with respect to the ϕ_T values of several (carbonyl) psoralens. **5** and **9** were first reported to have ϕ_T values of 0.45 and 0.14, respectively, in water; also, some triplet spectra obtained from pulse radiolysis appear to be different from those from flash experiments.[1] **9** and **7** were reported to have ϕ_T of 0.03 and 0.09, respectively, in methanol.[3] About the same time, still different values were reported of 0.06 for **5** and 0.04 for **9** in ethanol.[2] If the same absorption coefficients for the triplets were used

Table 2 Photophysical properties of psoralen derivatives and thione analogues (in methanol at 295 K except where noted)

	λ_{max}/nm[a]	$\lambda(T)_{max}$/nm[b]	ϕ_T	τ_T/μs	ϕ_Δ	F-P max/nm	τ_F/ns
5	330	425	0.10	4.8[c]	—	430 (F)	0.20[d]
6	380	510	0.58	1.6[c,e]	—	470 (F)?	—
						592 (P)	
9	*ca.* 340 (sh)	*ca.* 370[f]	⩽0.02 (Bz)	3.1[g]	—	480 (F)	0.45[h]
	300						
11	*ca.* 343 (sh)	*ca.* 405	—	0.7[i]	—	—	—
	307						
10	379	500	0.60	1.1[j]	0.70	*ca.* 450 (F)[k]	—
						591 (P)	
13	*ca.* 350 (sh)	400	—	1.9[c]	—	485 (F)	—
	310	*ca.* 450					
7	335	480[l]	0.26	5.3[c]	—	431 (F)	0.80[m]
8	400	510	—[n]	2.5[c,j]	—	*ca.* 460 (F)	—
						574 (P)	
15	*ca.* 325 (sh)	*ca.* 310	—[o]	0.8[p]	—	—	—
16	341	410, 530[q]	—	10.3[q]	—	440 (F)	—
14	*ca.* 340 (sh)	380[r]	—	5.3[s]			

[a] Longest-wavelength maximum of a $\pi \rightarrow \pi^*$ type transition. [b] All distinguishable $T \rightarrow T_n$ transition maxima are given with excitation at 355 nm. [c] At initial $A \leqslant 0.2$ and input energy <3 mJ. Recovery time same as decay time for **6**, **10** and **8**. [d] ±0.04. If not extensively purified, a second longer component contributing *ca.* 10% of the signal exists. [e] Extrapolated to zero concentration, lifetime was 1.3 μs at initial $A = 0.2$ and input <3 mJ, see text. [f] Because of the weak signal and broad spectrum, the maximum is not clearly defined and there may be one at longer wavelength. [g] In ethanol, $\tau = 4.0$ μs and in [$^2H_1$]ethanol, $\tau = 3.1$ μs at the same low initial A for all (*ca.* 0.18). [h] ±0.04 ns, 97% contribution and 9% contribution of a second component of $\tau = 0.91 \pm 0.01$ ns. [i] At input energy of ⩾25 mJ otherwise signal too weak to obtain decay data ($A = 0.18$). [j] Recovery lifetime is the same as the decay lifetime at 3–5 mJ input and initial A of 0.26. [k] The assigned fluorescence is somewhat questionable because of the weak signal. [l] Another maximum exists at *ca.* 370 nm which may represent another T–T transition. [m] ±0.10 ns, 93% contribution, and perhaps a 7% contribution of a second component of unknown origin $\tau = 2.71 \pm 0.63$ ns. Fluorescence maximum at 399 nm in cyclohexane. [n] The intensity of the T–T signal at the maximum is *ca.* 5 fold greater than that of **7** at the same initial A and input energy (20 mJ). [o] Literature data[1] give 0.009 in benzene and 0.33 in water, for ϕ_T; see text for our estimate. [p] Triplet lifetime with 20–25 mJ input and initial $A = 0.21$. Absorption proceeds to longer wavelength. [q] Two absorption maxima are nearly equally intense. Lifetime at ⩽3 mJ input and initial $A = 0.25$. Signal intensity 7–8 fold greater than that for **15**; see text for ϕ_T estimate. [r] Bands also occur at longer wavelengths (480, 650 nm). [s] Initial A 0.18 and ⩽3 mJ input.

for H_2O (as found in ethanol), then **5** and **9** would have ϕ_T values of 0.12 and 0.06, respectively,[2] in water (*cf.* the values of 0.45 and 0.14 found earlier). Also, despite a seeming agreement between 0.04 in ethanol and 0.03 in methanol for **9** the value of 0.03[3] was calculated from an apparently erroneous published absorption coefficient[1] and in fact, ϕ_T should be 0.01 using the new value.[2] Very recent data in 1,4-dioxane and 1,4-dioxane–water mixtures indicate that ϕ_T changes substantially for **5** as a function of water concentration (also true for **13** but much less so for **9**[33]). The values for ϕ_T for **5** and **9** in 1,4-dioxane are 0.04 and ⩽0.01 (*ca.* 0.5 and *ca.* 0.01–0.02 in water).[32] Our data in methanol give ϕ_T of **5** to be 0.10 and **9** to be ⩽0.02 in benzene while the TMP derivative is 0.26 in methanol (Table 2).

13 has been reported to have a ϕ_T of 0.1 in ethanol.[32] Based on our signal intensity and other factors, we would estimate a ϕ_T ⩽0.03 for **13** in methanol. Very recent data in solvent systems as above indicate that in pure 1,4-dioxane ϕ_T ≈0.08, then increases substantially to *ca.* 20% water and then decreases to near 0.01 in 70% water. In acetonitrile a value of 0.27 was found. The implication for **5**, **9** and **13** is that ϕ_T is a function of the composition of 1,4-dioxane–water mixtures, or the relative permittivity of the pure solvent.[32]

In summary, it would appear that there is some solvent dependence for ϕ_T but the magnitude is difficult to assess because of uncertainty in some of the ϕ_T values. The ϕ_T of **5** would seem to be in the range 0.06–0.09 in methanol or ethanol (0.04 in 1,4-dioxane and increasing with concentration of water to *ca.* 0.5), for **9** the ϕ_T range would appear to be 0.01–0.03 in methanol, ⩽0.02 in benzene and perhaps higher (0.04) in ethanol (⩽0.01 in 1,4-dioxane). For **7** ϕ_T is between 0.1 and 0.26 in methanol and is reported to be 0.21 in benzene.[33] For **13** there appears to be a marked solvent dependence for ϕ_T with values of *ca.* 0.1 in ethanol,[34] ⩽0.03 in methanol (our estimated data), *ca.* 0.08 in 1,4-dioxane,[32] 0.27 in acetonitrile and <0.01 in water.[31]

The triplet lifetimes of all psoralens range within the extremes of *ca.* 1–5 μs (extremes for **11** and **7**, respectively) (Table 2).

Others[30,31] have studied the emission of some psoralens in ethanol at 77 K. Our fluorescence data for **5** and **7** are similar (*ca.* 12 nm red shifted for ours in methanol at 298 K). However, our maximum of fluorescence of **9** is some 40 nm red shifted. Given the severe overlap seen by others between the fluorescence and phosphorescence, at 77 K, we believe the fluorescence maximum is at longer wavelength than was estimated.[30] In the case of **5** and **9**, fluorescence data[30] indicate the lowest excited singlet state is of (π, π^*) character. Based on our earlier consideration of energy difference criterion for assignment of these, we could not assign the n, π^* state as lowest. It was also believed[30] that the fluorescence lifetime of coumarin (the main moiety in psoralens) would be only *ca.* 0.1 ns based on the ϕ_F, f, and radiative lifetime. Furthermore, given the comparative ϕ_F and f values of the first transition of **5**, it is predicted that the fluorescence lifetime of **5** then would be *ca.* 0.02 ns. We found the lifetime for **5** to be 0.2 ns (in fluid solution, 298 K); moreover, the lifetime for **9** is 0.45 ns. Thus predicted values need to be considered with some scepticism. All lifetimes of the psoralens were <1 ns.

For the isopsoralens, literature data for **15** give values of 0.009 and 0.33 for ϕ_T in benzene and water, respectively.[1] Based on the reported ε_T values of **15** and **5** and our data on signal strengths (and initial absorbances and input energies), we predict ϕ_T to be *ca.* 0.05–0.1 for **15** in methanol. Note that at the same initial absorbance but at about one-eighth the energy input, the triplet signal of **16** is nearly equal to that of

Table 3 Comparison of experimental and theoretical transitions (in nm) for psoralens and thione analogues

	experimental[a] ($\varepsilon/10^4$ dm^3 mol^{-1} cm^{-1})	theoretical[b] INDO	theoretical[b] PPP
5		363 (0.001; n, π^*)	
	330	355 (0.30)	327 (0.23)
	292	316 (0.33)	302 (0.50)
	ca. 260 (sh)	264 (0.69)	260 (0.47)
	247	256 (0.15)	243 (0.73)
	ca. 215	232 (0.36)	225 (0.06)
		216 (0.07)	218 (0.13)
		208 (0.15)	207 (0.24)
			201 (0.43)
6		549 (0.0002; n, π^*)	
	381 (1.84)	403 (0.61)	371 (0.61)
	ca. 340 (sh)	338 (0.14)	336 (0.34)
	290 (sh)	286 (0.42)	289 (0.11)
	279 (sh)	279 (0.02)	271 (0.77)
	265 (3.34)	273 (0.04)	243 (0.13)
	242 (sh)	246 (0.60)	223 (0.21)
	ca. 223 (3.27)	233 (0.65)	219 (0.36)
		225 (0.22)	207 (0.36)
			203 (0.10)
9[c]		360 (0.001; n, π^*)	
	ca. 340 (sh)	358 (0.11)	
	300	327 (0.55)	
	ca. 265 (sh)	271 (0.16)	
	248	262 (0.70)	
	ca. 215	235 (0.14)	
		233 (0.22)	
		226 (0.20)	
		215 (0.04)	
		207 (0.10)	
11	*ca.* 343 (sh)		
	307		
	267		
	247		
	ca. 215		
10	378 (1.53)		
	ca. 340 (sh)		
	296 (sh)		
	269 (1.65)		
	226 (2.86)		
13[d]	*ca.* 350 (sh)		354 (0.49)
	310		312 (0.16)
	268		262 (0.75)
	249		246 (0.37)
	220		221 (0.16)
			207 (0.15)
7	335		
	295		
	ca. 260 (sh)		
	249		
8	401 (1.89)		
	ca. 340 (sh)		
	290 (sh)		
	269 (1.54)		
	240 (sh)		
	288 (3.44)		
	ca. 225		
15		360 (0.001; n, π^*)	
	ca. 325 (sh)	347 (0.18)	323 (0.35)
	300	326 (0.45)	289 (0.30)
	247	274 (0.28)	252 (0.35)
	ca. 215	251 (0.34)	245 (0.65)
		236 (0.22)	223 (0.15)
		230 (0.31)	210 (0.30)
		203 (0.48)	203 (0.14)
16		342 (0.0009; n, π^*)	
	341	341 (0.08)	351 (0.40)
	303	293 (0.30)	301 (0.15)
	264	272 (0.36)	255 (0.10)
	248	254 (0.50)	254 (0.81)
	216	244 (0.45)	240 (0.20)
		224 (0.23)	218 (0.22)
		203 (0.38)	214 (0.58)
			201 (0.46)

[a] Transitions (in nm) are to π, π^* states unless otherwise noted. [b] Oscillator strengths are in parenthesis; transitions for π, π^* unless otherwise noted. [c] The absorption spectrum of **14** is very similar to that of **9**, also see Table 2. [d] Calculation uses OH instead of OCH_3.

15. If they have about the same ε_T then ϕ_T of **16** is in the 0.5 range. Also note the considerable increase in the lifetime of the triplet of **16** (the methoxy derivative of **15**) compared to **15**, *ca.* 12 fold, whereas methoxy substitution of **5** to give **9** or **13** causes a decrease in the lifetime of the triplet. The methoxy substitution in the isopsoralen **15** also seems to produce a notable increase in ϕ_T which does not appear to occur for the psoralen structure.

Theoretical Calculations of State Energy Order : Thione Psoralens

For the thione psoralens, there appear to be five to seven $\pi \rightarrow \pi^*$ transitions between 450 and 220 nm. Theory predicts seven to eight transitions down to *ca.* 220 nm and one or two more to 200 nm. Experimentally, there is a significant red shift found for the two lowest $\pi \rightarrow \pi^*$ transitions compared with the carbonyl psoralens (Fig. 2, Tables 2 and 3), ranging from 40 nm, 3000 cm^{-1} (**10**) to 65 nm, 4500 cm^{-1} (**8**) which are similarly predicted by theory (Tables 2 and 3). This is expected from the greater conjugative interaction of sulfur compared to oxygen.[29] The first $\pi \rightarrow \pi^*$ transition is vibrationally resolved to some extent which is totally lacking for the carbonyl psoralens (Fig. 2).

In all cases, an $n \rightarrow \pi^*$ transition is predicted to be below the lowest $\pi \rightarrow \pi^*$ transition and considerably below the $n \rightarrow \pi^*$ of the psoralens, some 9000 cm^{-1}, Table 3. We were able to see a shoulder in the 470–550 nm region for **6**, we estimate a maximum at *ca.* 480 nm ($\varepsilon \approx 100$ dm^3 mol^{-1}

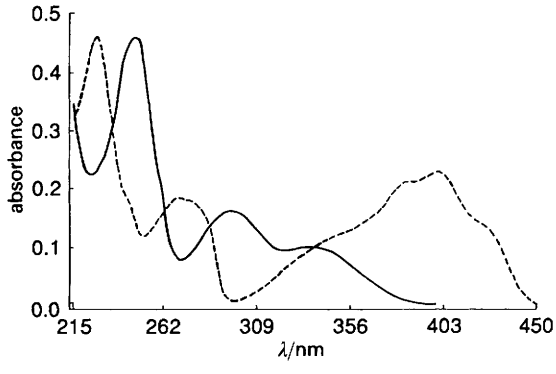

Fig. 2 Absorption spectra of **7** (——) and **8** (– – –) in methanol at 295 K

cm^{-1}) in toluene. We assign this to an n → π* transition. This is 2600 cm^{-1} higher than predicted but still clearly below the lowest π → π* transition as predicted, Table 3. The substantial lower energy of the n → π* transition of the thione psoralens compared to the psoralens is primarily the result of the much lower ionization energy of the n-orbital electrons (moving the n-orbital energy much closer to the π* orbital).[29]

There is excellent agreement regarding transition energies between theory and experiment using the PPP approximation (Table 3); it is also, good for INDO. Thus theory is very valuable in predicting the spectral properties of interest for the thione psoralens and their differences from the carbonyl psoralens.

Photophysical : Thione Psoralens

For the thione psoralens, the triplet maxima are red shifted which is particularly noticeable for **6** compared to **5** (Table 2) and for the same reasons given for the red shift in the π → π* singlet transitions. Comparing **8** with **7** there is little shift, and for **10** compared to **9**, it is uncertain because a weak band may be in the longer-wavelength region for **9**. Clear ground-state depletion spectra are seen for the thione derivatives (see, *e.g.* Fig. 3).

There is a very significant increase in ϕ_T for the thione derivatives compared to the carbonyl ones (Table 2). This ranges from *ca.* 6- to *ca.* 30-fold increase. We also measured ϕ_Δ for **10** and found it to be essentially the same as ϕ_T (Table 2). This indicates that there is approximately 100% energy transfer (to ground-state oxygen) in methanol. For **9** and **7** ϕ_Δ was reported to be *ca.* three-fold lower in magnitude than ϕ_T[36] or 35–45% energy transfer in benzene (for other psoralens, such as **13**, the efficiency was also low but was reported to be much higher for 3-ethoxycarbonyl psoralen and some psuedopsoralens). Others[9,11,37] have noted highly efficient energy transfer from some quite different thiones to generate singlet oxygen.

Table 2 gives data on the room-temperature fluorescence of the carbonyl psoralens; furthermore, there is data on the fluorescence and the unusual observation of phosphorescence in solution at room temperature. As noted in the Introduction, phosphorescence under similar conditions by other thione compounds is well known (see *e.g.* ref. 4 and 12).

For the thione psoralens, fluorescence was clearly observed for **8** but was much weaker and somewhat uncertain for **10**. Based on calculations, the $^1(n, \pi^*)$ state is expected to be considerably below the lowest $^1(\pi, \pi^*)$ state (*ca.* 6500 cm^{-1}, Table 3). Given the location of the fluorescence observed (Table 2), (maximum *ca.* 460 nm), it appears that the fluorescence originates from the upper $^1(\pi, \pi^*)$ state (S_2). This also appears to be the case for **8** (Fig. 4, Tables 2 and 3) (and for 8MOTP, but here the fluorescence was questionable). As noted above, the observation of fluorescence from S_2 of some thiones is well known (*e.g.* ref. 4 and 12). The occurrence of phosphorescence was verified by the substantial quenching of this emission in the presence of air compared to argon. The phosphorescence intensity could be largely recovered again by bubbling argon into the solution after the air and Fig. 4 shows the case of **8** in argon and in air. The phosphorescence was quenched four-fold in air compared to argon. Air quenching of the phosphorescence occurred for all of the thione psoralens. For **10** and **6**, the phosphorescence maxima and origins were the same within error, 591 and 592 nm, respectively. The maximum for **8** was blue shifted by 15 nm. The onsets of phosphorescence for all seem to be within the range 540–560 nm and determining any differences was not possible because of the error in determining onsets that overlap tail fluorescence. Based on the phosphorescence onset data, we were able to establish that all of the lowest triplets were located in the 18 250 cm^{-1} region.

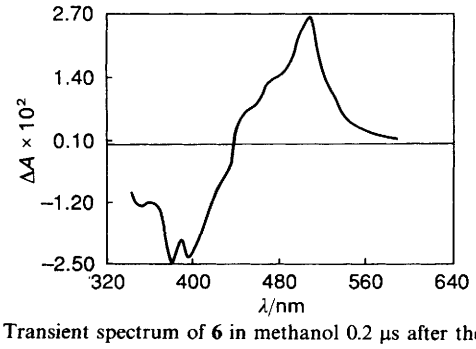

Fig. 3 Transient spectrum of **6** in methanol 0.2 μs after the flash at 295 K

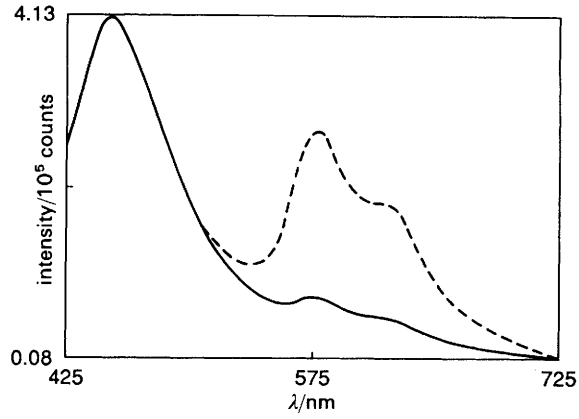

Fig. 4 Emission spectra of **8** in methanol with Ar (– – –) and with air (——) at 295 K. Emission at *ca.* 550–725 nm is phosphorescence.

Coumarins and Thione Coumarins

Compounds **1–4** were studied and a summary is given in Table 4. ϕ_T of **1** was measured in benzene by the energy-transfer method (to β-carotene) since no ground-state depletion was observed in methanol (or in benzene). Table 5 provides information on the comparison of theory and experiment regarding transition energies/wavelengths, their intensities and orbital origin assignments.

Theoretical Calculations of State Energy Order : Coumarins

The next group of compounds to be considered will be the coumarins. The lowest π → π* transition energy of **1** and **3** are significantly different, there being a 100 nm (7500 cm^{-1}) red shift for **3** (Fig. 5, Tables 4 and 5). We calculated results for C153, C152 and C151 (INDO), all of which have a CF_3 group in the same position and an amino (C151), alkylamino (C152), or cyclic amino-type substitution in the same position (see Fig. 1 for C153) and all had the same predicted S_1 energy within 150 cm^{-1}. Thus all of these are predicted to be red shifted by *ca.* 110 nm (7600 cm^{-1}) from coumarin (**23**), in excellent agreement with experiment (Tables 4 and 5). In this case, the red shift compared to coumarin is the result of the type of substitutions which not only introduce significant conjugative effects but also substantial change-transfer character. Furthermore, the first transition of **3** is very broad, 80 nm (4300 cm^{-1}) at half maximum intensity. Theory (INDO) predicts two intense close-lying transitions at 444 and 403 nm (Table 5), therefore, it is very like the experimentally observed band at 422 nm is an unresolved combination of the two transitions.

Table 4 Triplet state and ϕ_Δ properties of coumarins and thione analogues (in methanol at 295 K except where noted)

	λ_{max}/nm[a]	$\lambda(T)_{max}$/nm[a]	ϕ	τ_T/μs	ϕ_Δ	F-P max/nm
1	321	420	0.04 (Bz)	2.3[b] (7 μs, Bz)	—	*ca.* 370 (F)[c]
2	379	480	0.75	1.4[d]	0.70	*ca.* 450 (F)[e] 595 (P)
3	422	490–770[f] (Bz)	⩾0.02 (Bz)	25 (Bz)[f]	—	—
4	514	320, 670–760[g]	—[g]	6.0[g]	—	—

[a] See Table 2. [b] Lifetime at $A = 0.16$ and input energy ⩽3 mJ. Bz is benzene. [c] This is in 1,4-dioxane with a lifetime of ⩽0.3 ns. [d] Same lifetime for ground-state recovery, at $A = 0.32$ and 5 mJ. [e] Fluorescence is questionable, although weak emission was seen at both 295 and 77 K. [f] This is the total of the broad very weak band and a maximum could not be determined. Our lifetime is considerable longer than that obtained by pulse radiolysis of a benzene solution (half-life, 5 μs). [g] Initital $A \approx 0.01$ and 1 mJ. The band in the red region is very broad (540 to >800 nm) and constant over much of this region so the maximum is uncertain. Decay at 670 nm and recovery have same lifetime. In toluene, the spectrum and lifetime are similar. The triplet and depletion signals at the same initial A and input energy as **3** are ⩾80 times greater. Taking into account the difference in absorption coefficient (Table 5) and assuming this is similar for the triplet, the ϕ_T can be estimated to be ⩾0.8.

For coumarin, INDO and PPP are in good agreement for all of the transitions (Table 5). For C153 (C152 and C151), no transitions of oscillator strength ⩾0.05–0.07 are predicted from 400 to 260 nm.

Finally, for both **1** and C153 (and C152 and C151), n → π* transitions are predicted (by INDO) to be definitely below the lowest π → π* transition (Table 5) (*i.e.* barely below those for the psoralens, Table 3). The lowest ^{1}(n, π*)–(π, π*) separations for C153, C152 and C151 (270 nm, 8500 cm^{-1}) are predicted to be substantially greater than for the parallel separation for coumarin (32 nm, *ca.* 2700 cm^{-1}) and the (carbonyl) psoralens in general; moreover, this is also true for **4** and thione psoralens (Tables 3 and 5). Although we cannot be certain why this is true, it appears to originate in the significant introduction of of charge-transfer interaction in the C151, C152 and C153 molecules.

We were unable to observe an n → π* transition in **1** even when the absorbance at the long-wavelength maximum was >4.5.

Table 5 Comparison of experimental and theoretical transitions (in nm) for coumarins and thione analogues

	experimental[a] (ε/10^4 dm^3 mol^{-1} cm^{-1})	theoretical[a] INDO	theoretical[a] PPP
1[b]		364 (0.0008; n, π*)	
	321	332 (0.47)	317 (0.39)
	275	298 (0.18)	275 (0.14)
	235	240 (0.16)	234 (0.39)
	ca. 215	235 (0.25)	226 (0.35)
		209 (0.67)	214 (0.42)
2[c]	*ca.* 480 (0.005)	569 (0.0002; n, π*)	
	379 (1.66)	400 (0.65)	369 (0.63)
	315 (0.55)	310 (0.06)	309 (0.05)
	274 (1.05)	279 (0.15)	275 (0.42)
	ca. 247 (1.18)	251 (0.24)	254 (0.13)
	ca. 214	219 (0.19)	244 (0.37)
		215 (0.24)	215 (0.20)
			211 (0.11)
			203 (0.62)
3[d]		712 (0.006; n, π*)	
	423 (1.47)[d]	444 (0.38)	
	ca. 315 (sh)	403 (0.44)	
	ca. 290 (sh)	397 (0.05)	
	266	370 (0.05)	
		297 (0.07)	
4	514 (2.37)[e]		
	375 (0.46)		
	ca. 310 (sh)		
	284 (1.84)		
	257 (3.06)		
	ca. 212		

[a] See Table 3. [b] The experimental data are for **1** while theory is for **23**. The transition at 235 nm occurs only as a very weak band in a minimum and the band location of the shortest-wavelength transition is uncertain. [c] Experimental data are for **2** while theory is for **24**. [d] The observed band at 423 nm is unusually broad, *ca.* 80 nm at one-half intensity maximum. It may well be composed of two close-lying transitions as indicated by theory (444 and 403 nm)(ε = 1.53 × 10^4 dm^3 mol^{-1} cm^{-1} in toluene). The band at 315 nm is weak and 290 nm is a shoulder. Also, if the cyclization to the N is removed and only NH_2 is present, now coumarin 151, or $N(CH_3)_2$ is present, now coumarin 152, the theoretical data are very similar (although the second transition is blue-shifted by *ca.* 14–17 nm). No further transitions are predicted to 200 nm with $f \geqslant 0.03$. [e] In acetonitrile and toluene, the values are 2.43 × 10^4 and 2.87 × 10^4 dm^3 mol^{-1} cm^{-1}, respectively.

Theoretical Calculations of State Energy Order : Thione Coumarins

2 has its first π → π* transition maximum red shifted by 60 nm (4800 cm^{-1}) from **1** (Fig. 5). Theory is in good agreement regarding both the magnitude of the shift (from **1**) and in predicting the right order of intensity for the first two transitions of **2** (Table 5). The reason for the red shift is the same as that given earlier for the psoralens and thione psoralens.

For **2**, a ^{1}(n, π*) state (569 nm) is predicted to be at much lower energy, 7500 cm^{-1} than the first ^{1}(π, π*) state (400 nm). Moreover, the (n, π*) state is predicted to be at much lower energy, 10 000 cm^{-1}, than the (n, π*) of **1** (364 nm), Table 5. Experimentally in toluene we were able to observe a shoulder in the 470–550 nm region of **2**; we estimate a maximum near 480 nm. We assign this to an n → π* transition (ε ≈ 55 dm^3 mol^{-1} cm^{-1}). This is 3000 cm^{-1} higher in energy than pre-

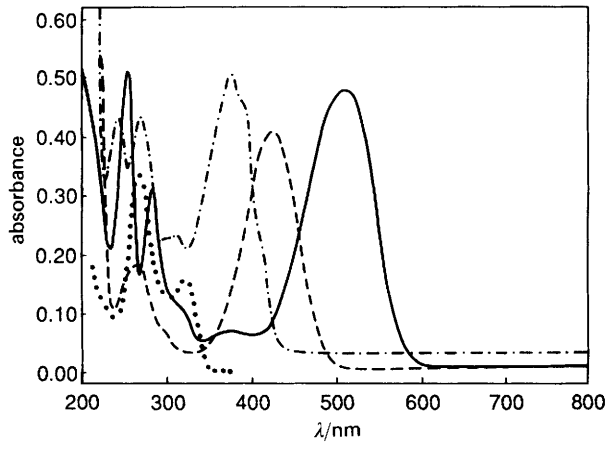

Fig. 5 Absorption spectra of **1** (· · ·), **2** (– · –), **3** (– – –) and **4** (——) in methanol at 295 K

dicted but nonetheless is significantly lower in energy than the lowest $\pi \rightarrow \pi^*$ transition, as predicted (Table 5). Others[38] assigned a shoulder in the *ca.* 490 nm region in **24** to an $n \rightarrow \pi^*$ transition.

Although no INDO calculation was made for **4** it is clear, based on the shift of the $n \rightarrow \pi^*$ transition between **1** and **2** (10 000 cm^{-1} red shift), that the $n \rightarrow \pi^*$ transition for **4** should be in the 900 nm region, in the near-infrared. Based on predictions compared with experiments for **17**, **18** and **20** theory predicts the $n \rightarrow \pi^*$ transition to be 3000–6000 cm^{-1} lower in energy than is found by experiment (see later discussion). Nonetheless, the $n \rightarrow \pi^*$ transition of **3** is still expected to be in the near-infrared region. A low-lying $\pi \rightarrow \pi^*$ transition (514 nm) is observed for the **4** (Fig. 5, Tables 4 and 5), that is red shifted by 90 nm (4200 cm^{-1}) from that of **3** for the reason discussed above. This red shift is 30 nm greater (but approximately the same energy difference) than the red shift for **2** compared to **1**.

The first transition of **2** strongly resembles that of **6**, both in location (Tables 2 and 4) and shape. Other similarities regarding ϕ_T triplet lifetime, ϕ_Δ, fluorescence and phosphorescence will be noted later.

Photophysical: Coumarins and Thione Coumarins

The absorption and fluorescence of **23** and **1** at 77 K in ethanol and their theoretical properties for **23** have been studied.[31,32] **23** and **1** fluoresce at 77 K but **23** does not fluoresce at room temperature. No fluorescence was observed for **23** and **1** in methanol at room temperature.[39] However, we observed fluorescence of **1** at room temperature in 1,4-dioxane and obtained a lifetime of $\leqslant$0.3 ns (>98%) (Table 4). For **23**, our theoretical data are in slightly better agreement regarding transition energies. Also, we predict that an n, π^* state exists and that it is somewhat lower in energy; however see the earlier discussion regarding assignment of n, π^* and π, π^* state order. Based on these we cannot assign the n, π^* state as the lowest in methanol but it is probably so in non-polar solvents. Fluorescence data[40] suggest that the lowest excited state is of (π, π^*) type in a polar solvent at 77 K.

ϕ_T for **1** is quite low (*ca.* 0.04) but it is dramatically enhanced in **2** (0.72; Table 4), as expected. Again, as for the carbonyl and thione psoralens, the T–T absorption maxima are red shifted going from carbonyl to thione. In the case of the triplet lifetimes, there is a significant decrease going from carbonyl to thione, especially for **3** *cf.* **4** (Table 4). This qualitative trend in triplet lifetimes is also present in the psoralen analogues. For **2** we measured ϕ_Δ and found it to be essentially identical to ϕ_T, again indicating *ca.* 100% efficient energy transfer as for the thione psoralens ($S_\Delta \approx 1$).

Only fluorescence was observed for **1** at room temperature in solution. However, for **2** phosphorescence with a maximum near 600 nm with an onset at *ca.* 560 nm (51.0 kcal mol^{-1}) was clearly observed in argon-saturated solution (Table 4), which is very similar to that of a thione psoralen (Fig. 4). The latter was quenched by air, but not completely (a questionable fluorescence may exist also). The lowest triplet state energy of **2** is (*ca.* 560 nm) 17 860 cm^{-1}, similar to the thione psoralens.

The ϕ_T and triplet lifetime of **2** are similar to **6** and **10**. Based on ϕ_T and ϕ_Δ data of the thione psoralens and coumarins, we expect all of the thione psoralens to have ϕ_T and ϕ_Δ in the 0.6–0.9 range and S_Δ to be *ca.* 1. The triplet lifetimes of all thiones are expected to be 1–3 μs. All the data indicate a very significant resemblance of thione coumarins (**2**) to thione psoralens regarding the lowest transition energy (and some other transitions), ϕ_T, ϕ_Δ, S_Δ, triplet lifetime and lowest triplet state energy (based on phosphorescence maxima and onsets). This is somewhat surprising since it indicates that the addition of a double bond and alkoxy-type substitution (the furan ring) has little consequence on the lowest transition energy or photophysical properties of **2**. Some of the above is also true for the comparison of **1** with **5**.

Others have examined the parent thione coumarin **24** (called an enethione).[5] They found results very similar to ours (in methanol) regarding the lowest triplet-state energy of 212 kJ mol^{-1} [based on low-temperature (77 K) phosphorescence data] *cf.* our 214 kJ mol^{-1} (51.0 kcal mol^{-1}). Also, triplet-state properties of $\phi_T \approx 0.9$ (±20%) *cf.* our 0.75, ϕ_Δ of 0.8 (±25%, excitation into the π, π^* state; higher upon excitation into the n, π^* state, 1.0) *cf.* our 0.70, and a triplet lifetime of $\geqslant$2.5 μs (τ_0 ±15%) *cf.* our 1.4 μs (low absorbance and input energy) were similar. There was apparently no attempt made to observe phosphorescence at room temperature. They also found a large self-quenching rate constant (9×10^9 dm^3 mol^{-1} s^{-1}) and a high oxygen quenching rate constant of 3×10^9 dm^3 mol^{-1} s^{-1}.

Chromones

Compounds **17**–**22** were examined and a summary is presented in Table 6. ϕ_T values of **21** and **19** were measured in benzene by the energy-transfer method (to β-carotene) since no ground-state depletion was observed in methanol.

Theoretical Calculations of State Energy Order : Chromone and Thione Chromone

The next group of compounds of concern are those containing a chromone or thione chromone moiety. Tables 6 and 7

Table 6 Triplet state and ϕ_Δ properties of chromones and thione analogues (in methanol at 295 K except where noted)

	λ_{max}/nm[a]	$\lambda(T)_{max}$/nm[b]	ϕ_T	τ_T/μs	ϕ_Δ	F-P max/nm
17	296	630[c]	—[c]	0.20[d]	—	no F[e]
18	371[f]	460	—	0.23[g]	—	660 (P)[h]
21	323	380[i]	0.70 (Bz)	25[j]	0.20	—
22	385[f]	—[k]	—	—	—	—
19	330	355[l]	0.71 (Bz)	70	0.25 (Bz)	500 (F)[m]
20	385, 357[f,o]	—[k]	—	0.1[n]	—	—

[a] See Table 2. Also $n \rightarrow \pi^*$ transitions occur at longer wavelength for **17**, **18**, **20** and **22**; see Table 7. [b] See Table 2. [c] In acetonitrile this extends to 380 nm, excitation 266 nm. Others[41] give a ϕ_T of 0.9–1 (±15%). [d] Lifetime in acetonitrile is considerable longer, 1.1 μs, input energy <3 mJ (266 nm) and initial $A = 0.2$. [e] No fluorescence was observed at room temperature, $\phi_F \leqslant 0.003$. [f] A weak $n \rightarrow \pi^*$ transition occurs with a maximum at *ca.* 525 nm for **18** and *ca.* 495 nm for **20** and **22**. [g] Lifetime in acetonitrile is considerably longer, 1.8 μs, input energy $\leqslant$3 mJ (355 nm) and initial $A = 0.26$. [h] These are room-temperature data in acetonitrile by laser flash. Recovery of the phosphorescence signal had a lifetime the same as the triplet decay of 1.8 μs, see footnote *g*. [i] Another very broad absorption occurs to longer wavelength with a maximum in the region 610–660 nm. [j] Initial $A = 0.7$ at 355 nm, input energy 4.5 mJ. [k] No authentic T–T absorption spectrum could be obtained for **22** with a high laser energy input ($\geqslant$35 mJ beam and $A = 0.8$ at 355 nm). A weak T–T signal was monitored at 525 nm for **20** in order to obtain τ_T (input energy $\geqslant$20 mJ, initial $A = 0.3$). [l] Another very broad absorption occurs to longer wavelength with a maximum in the region 610–660 nm; for lifetime, input energy $\leqslant$3 mJ and initial $A = 0.21$. [m] Khellin has a fluorescence lifetime of 0.30 ± 0.04 ns. [n] May be limited by instrument time resolution. [o] These bands are of nearly equal intensity whereas the one at *ca.* 357 nm is clearly weaker in **22**.

Table 7 Comparison of theoretical and experimental transitions (in nm)

	experimental[a] ($\varepsilon/10^4$ dm^3 mol^{-1} cm^{-1})	theoretical[a] INDO	theoretical[a] PPP
17[b]	330 (n, π^*)[b]	418 (0.0000; n, π^*)	
	296, 303 (sh)	290 (0.09)	296 (0.32)
	239	249 (0.12)	266 (0.06)
	ca. 215	244 (0.35)	244 (0.29)
		225 (0.42)	237 (0.38)
			206 (0.55)
18	530 (n, π^*)[c]	632 (0.0000; n, π^*)	
	371 (1.63)	356 (0.52)	357 (0.62)
	ca. 300 (sh)	300 (0.04)	295 (0.21)
	277 (0.79)	286 (0.09)	281 (0.17)
	242 (0.77)	277 (0.17)	233 (0.55)
	ca. 215 (2.2)	250 (0.05)	200 (0.48)
21		430 (0.0000; n, π^*)	
	323	330 (0.05)	318 (0.59)
	276	278 (0.01)	294 (0.21)
	257	257 (1.06)	254 (0.13)
	243	249 (0.25)	242 (0.25)
	210	242 (0.07)	223 (0.12)
		227 (0.26)	214 (0.43)
		211 (0.17)	204 (0.15)
22	500 (n, π^*)		
	385		
	350 (sh)		
	298		
	248		
19[d]		415 (0.0001; n, π^*)[d]	
	330	332 (0.06)	338 (0.12)[e]
	280	280 (0.07)	288 (0.43)
	250	257 (0.24)	261 (0.95)
	ca. 215	255 (0.85)	247 (0.17)
		238 (0.11)	235 (0.17)
		223 (0.55)	233 (0.41)
			211 (0.67)
20	496, 525 (n, π^*)[f]	682 (0.0000; n, π^*)[g]	
	385 (0.84)	384 (0.24)	
	357 (0.87)	354 (0.32)	
	298 (0.56)	299 (0.12)	
	260 (2.07)	284 (0.12)	
	ca. 249 (2.13)	274 (0.62)	
	ca. 215 (2.26)	241 (0.51)	
		229 (0.04)	

[a] See Table 3. [b] A weak series of three bands appears on the long-wavelength tail in benzene, 330 nm is the middle of the three. For $\pi \rightarrow \pi^*$ transitions, in acetonitrile 303, 238 and 215 nm and in benzene 305 nm. [c] ε for the n, π^* transition is 22 dm^3 mol^{-1} cm^{-1} in toluene and has a maximum at 561 nm. [d] Using, MMX data for **19** resulted in very similar results, 1–7 nm differences. [e] PPP calculations were performed using MMX data where the two methoxy groups were considered as hydroxy groups. [f] It is difficult to decide the maximum of three weak bands because of an adjacent band tail; these are the two bands at longest wavelength. [g] The two methoxy groups were taken as hydroxy groups (MMX data).

contain the experimental and theoretical results. **17** has its longest-wavelength absorption band maximum of $\pi \rightarrow \pi^*$ type near 300 nm (with two close-lying components) (Fig. 6). **23** shows more transitions in the same region and the longest-wavelength band is red shifted by *ca.* 20 nm (to 321 nm) compared to **17**. Both have predicted $n \rightarrow \pi^*$ transitions at longer wavelength (**17** longer, *ca.* 420 nm *cf.* 360 nm for **23**). Moreover, the $n \rightarrow \pi^*$ transition of **23** has been observed in the 340 nm region[41] and we believe we observed it in benzene (Table 7). A significant change in the spectrum occurs when going to **18**. The longest-wavelength $\pi \rightarrow \pi^*$ band is strongly red shifted to 370 nm (from *ca.* 300 nm in **17**), as expected. The spectrum is similar to that of **24** regarding transition locations and their numbers (Tables 5 and 7); this is not true for **17** compared to **23** (including intensities). An $n \rightarrow \pi^*$ transition is discernible in **18** near 530 nm (561 nm in toluene) which is predicted by INDO to be near 630 nm (*ca.* 420 nm predicted for **17**, 330 nm found). Similar results for **18** have been found by others regarding the experimental location of the n, π^* state.[4] The experimental red shift of the $n \rightarrow \pi^*$ transition of **18** from **17** is very large, *ca.* 11 000 cm^{-1}. In general, theoretical predictions are in very good agreement with experiment (Table 7), except for the $n \rightarrow \pi^*$ transition.

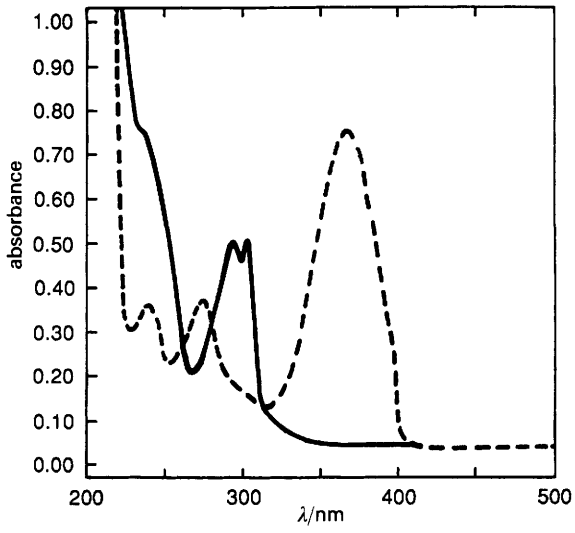

Fig. 6 Absorption spectra of **17** (——) and **18** (– – –) in methanol at 295 K

Photophysical : Chromone and Thione Chromone

17 shows a broad T–T transition (towards shorter wavelength) in the visible (maximum 630 nm) and the lifetime in acetonitrile is 1.1 μs but much shorter in methanol, 200 ns (Table 6). Others[41] have reported similar results (τ_0 = 1.8 μs in acetonitrile and 180 ns in methanol). **18** has a T–T transition with a maximum at 460 nm with clear depletion showing up by 400 nm (Fig. 7) and the lifetime is 1.8 μs in acetonitrile and again much shorter in methanol, 230 ns. Others[41] have demonstrated that high quenching rate constants exist for **17**, (3–4) × 10^9 dm^3 mol^{-1} s^{-1} and also that ϕ_T is high 0.9–1.0 (±15%). Note that our ϕ_T value for **23** is *ca.* 0.04, much less than that found for **17** (0.9–1). It is obvious that the structural difference in the heterocyclic ring has a dramatic effect. Based on the predicted location of the $n \rightarrow \pi^*$ transitions and the location of the longest-wavelength $\pi \rightarrow \pi^*$ transitions, it could well be that the lowest triplet state of **23** will be $\pi \rightarrow \pi^*$ while that of **17** will be n, π^* with a π, π^* state nearby (see later discussion).

For **18** we were able to observe phosphorescence at room temperature in acetonitrile during the flash experiment determining the T–T spectrum (Fig. 7); maximum at 660 nm (onset near 660 nm, 46 kcal mol^{-1}). The lowest triplet energy of **17** is *ca.* 75 kcal mol^{-1}).[42] The lifetime (of recovery) of the phosphorescence in acetonitrile of **18** was 1.8 μs, the same as the T–T absorption decay (Table 6). Phosphorescence has been observed at room temperature in an inert perfluoroalkane solvent with the same triplet energy.[4] The lifetime obtained in the absence of self-quenching in the inert solvent was 16 μs. For **2**, we determined the lowest triplet to be at *ca.* 51 kcal mol^{-1}. Thus, considering the small difference in the lowest singlet energies between **2** and **18**, the triplet state of **18** is located close to where it is expected compared with **2** and both are clearly lower in energy than **17**, but so are the lowest singlet states. Note also that the triplet

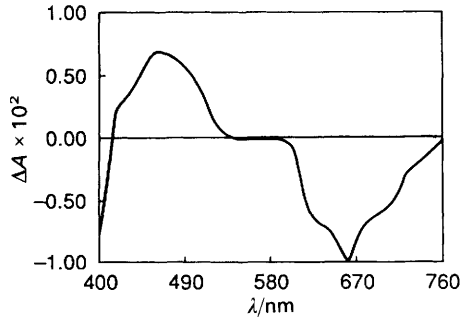

Fig. 7 Transient spectrum of **18** in methanol 0.4 μs after the flash at 295 K

lifetimes of both **1** and **2** are substantially longer than for **17** and **18** in methanol (Tables 4 and 6).

Based on the existence of very low lying (n, π^*) singlet states, and the comparative triplet lifetimes of **18** and **17**, it would be reasonable that the lowest triplet of **18** is (n, π^*) as it seems to be for **17**.

Theoretical Calculations of State Energy Order : Furochromones and Thione Furochromones

The other compounds to be considered are **19–22** (Tables 6 and 7), all of which contain the chromone (**19** and **21**) or thione chromone moiety (**20** and **22**). In all of the cases, either one or two methoxy groups exist on the central ring, in addition to the five-membered furan ring that has a methyl group (the furan ring is also present in psoralens). **21** (one methoxy group) and **19** (two methoxy groups) have very similar absorption spectra with a small red shift in **19**. We did not observe an n → π^* transition, although one is predicted for both and at very nearly the same wavelength as for **17** (Table 7). The PPP calculations are quite good regarding energies for **19** and **21**.

The thione counterparts **20** and **22** again show a strong red shift of the lowest-energy n → π^* transition by 40–60 nm (3000–5000 cm^{-1}) compared to **19** and **21** (Tables 6 and 7, and Fig. 8) and for the same reasons as given earlier. Partially structured n → π^* transitions were observed for **20** and **22** with maxima at 500–525 nm (fig. 8) (an unstructured n → π^* transition exists for **18** at *ca.* 525 nm).

Photophysical : Chromones, Furanochromones and Thiones

We recall that the ϕ_T of **17** is 0.9–1;[41] moreover, we have determined that both **19** and **21** have ϕ_T values of 0.7, similar to that of **17**. For **19** we also determined ϕ_Δ and found it to be clearly lower than 0.7 (0.25) (Table 6), indicating a 30–40% efficiency of energy transfer ($S_\Delta = 0.34$). This is parallel to the results for the carbonyl psoralens where the efficiency is also low, 35–45%, see earlier discussion. However, this low efficiency is not present for **10** or **2** and is probably not present for the thione psoralens and coumarins in general.

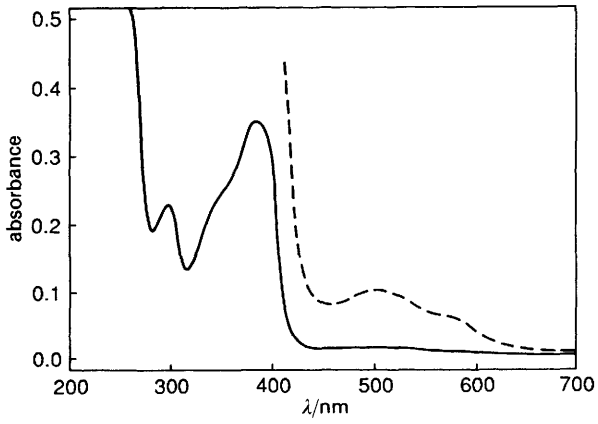

Fig. 8 Absorption spectra of **22** in methanol at 295 K at high concentration (– – –) and low concentration (——)

The triplet lifetimes of **19** and **21** (which contain chromone moieties) are 100–300 times longer than for **17** (Table 6). This is very different from the comparison of psoralens (which contain coumarin moieties) and coumarin (Tables 2 and 4), where **1** is comparable in lifetime with all of the psoralens (average 2–3 μs). If the lowest triplet state of **17** is (n, π^*) while that of **19** and **21** are (π, π^*), then the difference can be understood. Even in polar solvents the triplet state of **17** has substantial (n, π^*) character.[41] On the other hand, these comparisons and those of coumarin with the psoralens, suggests the lowest triplet state of all of the psoralens is dominantly of (π, π^*) type.

The surprise was the essential absence of any T–T absorption signal for **22** and **20** compared to the relatively high absorbance (and ϕ_T) for **21** and **19** for input energies of 3–4 mJ. Although we did not measure ϕ_T for **18**, there was an easily discernible T–T absorption signal. No signal could be seen for **22** even with input energies $\geqslant$35 mJ and initial absorbances up to 0.7 (a signal was seen for **20** with a focused 11 mJ beam). The lifetime for **20** was short, *ca.* 100 ns. These apparent results on ϕ_T going from **19** and **21** to **20** and **22** are in marked contrast to those obtained going from carbonyl psoralens to thione psoralens where there is a large increase in ϕ_T. It is possible that the lifetimes are so short that with our time resolution capabilities, we simply do not observe the main portion of the triplet signal (however, this is doubtful given the *ca.* 200 ns lifetime of **18** and *ca.* 100 ns for **20**). Also, based on the results of **2** and psoralens, it is expected that the lowest triplet state is located similarly for **18**, **20** and **22**, near 17 000 cm^{-1}. Note the lowest triplet of **2** (a thione coumarin) is similar in energy to that of **18** (thione chromone, 18 000 cm^{-1} *cf.* 17 000 cm^{-1}). It is clear that there is a low-lying ^{1}(n, π^*) state for **20** and **22** (and for **18**). Also, it is reasonable that the lowest triplet could be (n, π^*) Thus if there were little or no vibronic coupling of the ^{1}(n, π^*) and ^{1}(π, π^*) states because of the large energy separation, and if there were no ^{3}(π, π^*) states between the ^{1}(n, π^*) and ^{3}(n, π^*) states, to which the ^{1}(n, π^*) could directly couple, then coupling between ^{1}(n, π^*) and ^{3}(n, π^*) could be small and intersystem crossing in **20** and **22** could also be small.

In addition to learning more about the photophysical and photochemical properties of the carbonyl-type compounds, as well as the consequences of altering carbonyls to thiones for carbonyls we were interested in the photosensitizing activity of the thione compounds. We first wanted to predict which compounds might be active photosensitizers in biological systems and we wished to obtain experimental proof of the biological phototoxicity. This type of information is rarely known for newly developed, and often for older, photosensitizers.

Over the past years, a series of mutant *E. coli* strains differing in their sensitivity to inactivation by specific phototoxins/photosensitizers have been developed (*e.g.* ref. 16, 17, 35, 43). If a particular mutant strain is sensitive to inactivation by a particular photosensitizer, then the mutation must result in a modification that in the non-mutant strain must be important for the cell to respond to the particular photosensitizer. There are strains that test for the role of carotenoids in protecting against damage of a particular photosensitizer/phototoxin; there are also strains testing the role of catalase, superoxide dismutase and the importance of DNA as target sites. For example, an *E. coli* strain expressing carotenoids is protected from oxygen-dependent photosensitizers, such as λ-terthienyl, the principal target of which is the mem-

brane.[43,44] On the contrary, those strains not expressing carotenoids were not protected (*i.e.* the survival was $\geqslant 10^5$ lower at a given fluence and concentration of photosensitizer).[43]

In a cooperative effort, we have evaluated the biological photosensitizing ability of two of the compounds studied here (**2** and **10**).[45] This included not only phototoxic behaviour but also an evaluation of the target site(s) using mutant *E. coli* strains. Both were shown to have phototoxic character and **2** was highly active in the UV-A where **1** could not even be activated.

In conclusion, several successes of importance can be noted. We have been able to accomplish all of our goals regarding photophysical aspects by substitution of a thione for a carbonyl moiety. The absorption spectra have been shifted from the UV-C and UV-B into the UV-A or visible region and from the UV-A into the visible region. Both triplet and singlet oxygen quantum yields were increased, often significantly. Our theoretical calculations were successful in predicting significant long-wavelength shifts, particulary of the lowest-energy transition (which was the one most of interest) and did well for most other transitions). Finally, two of the thiones tested were photosensitizers and **2** was activated in the UV-A where **1** was inactive. Other tests involving fungi have shown that a number of the compounds are phototoxic even in the visible region, whereas the carbonyl counterparts are not.

References

1 R. V. Bensasson, T. J. Land and C. Salet, *Photochem. Photobiol.*, 1978, **27**, 273.
2 T. Sa Melo, D. Avenbeck, R. V. Bensasson, E. J. Land and C. Salet, *Photochem. Photobiol.*, 1979, **30**, 645.
3 D. C. Beaumont, R. J. Parsons, S. O. Phillips and J. C. Allen, *Biochem. Biophys. Acta*, 1979, **562**, 214.
4 R. P. Steer and V. Ramamurthy, *Acc. Chem. Res.*, 1988, **21**, 380.
5 K. Bhattacharyya, P. K. Das, V. Ramamurthy and V. P. Rao, *J. Chem. Soc., Faraday Trans. 2*, 1986, **82**, 135.
6 A. Maciejewski and R. P. Steer, *Chem. Phys. Lett.*, 1983, **100**, 540.
7 M. Maheney and J. R. Huber, *Chem. Phys. Lett.*, 1975, **30**, 410.
8 P. de Mayo, *Acc. Chem. Res.*, 1976, **9**, 52.
9 C. V. Kumar, H. F. Davis and P. K. Das, *Chem. Phys. Lett.*, 1984, **109**, 184.
10 A. Maciejewski, D. R. Demmer, D. R. James, A. Safarzadeh, R. E. Verrell and R. P. Steer, *J. Am. Chem. Soc.*, 1985, **107**, 2831.
11 V. Ramesh, N. Rammath and V. Ramamurthy, *J. Photochem.*, 1982, **18**, 293.
12 V. Ramamurthy, *Org. Photochem.*, 1985, **7**, 231.
13 F. Dall 'Acqua, *NATO ASI Ser. H15*, 1988, 269.
14 R. W. Tuveson, M. R. Berenbaum and E. E. Heininger, *J. Chem. Ecol.*, 1986, **12**, 933.
15 J. B. Hudson and G. H. N. Towers, *Photochem. Photobiol.*, 1988, **48**, 289.
16 R. W. Tuveson, in *Light Activated Pesticides*, ed. J. R. Heitz and K. R. Downum, ACS Symp. Ser. 339, 1987, pp. 192–205.
17 D. L. Klamen and R. W. Tuveson, *Photochem. Photobiol.*, 1982, **35**, 167.
18 R. S. Becker and K. Freedman *J. Am. Chem. Soc.*, 1985, **107**, 1477.
19 A. Grinwald and J. Z. Steinberg, *Anal. Biochem.*, 1974, **59**, 583.
20 A. E. McKinnon, A. G. Szabo and D. R. Miller, *J. Phys. Chem.*, 1977, **81**, 1564.
21 J. Carmichael and G. L. Hug, *J. Phys. Chem. Ref. Data.*, 1986, **15**, 1.
22 R. S. Becker, S. Das, S. Chakravorti and A. R. Morgan, *J. Photochem. Photobiol. B*, 1991, **10**, 345.
23 E. Gandin, Y. Lion and A. Van de Vorst, *Photochem. Photobiol.*, 1983, **37**, 279.
24 A. A. Gorman, I. Hamblett and M. A. J. Rodgers *J. Am. Chem. Soc.*, 1984, **106**, 4679.
25 J. E. Ridley and M. C. Zerner, *Theor. Chim. Acta*, 1973, **32**, 111.
26 R. Pariser and R. Parr, *J. Chem. Phys.*, 1953, **21**, 767.
27 R. Jutterman, D. Averbeck and S. Averbeck II, *Farmaco*, 1980, **40**, 3.
28 A. Schonberg and G. Schultz, *Chem. Bar.*, 1960, **93**, 1466.
29 R. S. Becker, in *Theory and Interpretation of Fluorescence and Phosphoresence*, Wiley Interscience, New York, 1969.
30 W. W. Mantulin and P-S. Song, *J. Am. Chem. Soc.*, 1973, **95**, 5122.
31 T. A. Moore, M. L. Harter and P-S. Song, *J. Mol. Spectrosc.*, 1971, **40**, 144.
32 T. Sa Melo, L. Riberiro, A. Macanita, M. Bazin, J. Ronford-Haret and R. Santus, *Int. Conf. Luminescence Spectroscopy*, Lisbon, 1990.
33 C. N. Knox, E. J. Land and T. G. Truscott, *Photochem. Photobiol.*, 1986, **43**, 359.
34 M. Craw, R. V. Bensasson, J. C. Ronford-Haret, M. T. Melo and T. G. Truscott, *Photochem. Photobiol.*, 1983, **37**, 611.
35 R. W. Tuveson, R. A. Larson, K. A., Marley, C. R. Wang and M. R. Berenbaum, *Photochem. Photobiol.*, 1989, **50**, 733.
36 T. Sa Melo, A. Macanita, M. Prieto, M. Bazin, J. Ronford-Haret and R. Santus, *Photochem. Photobiol.*, 1988, **48**, 429.
37 A. Safarzadeh, D. A. Condiaston, R. E. Verrell and R. P. Steer, *Chem. Phys. Lett.*, 1981, **77**, 99.
38 K. Bhattacharyya, P. K. Das, V. Ramamurthy and V. P. Rao, *J. Chem. Soc., Faraday Trans. 1*, 1986, **82**, 135.
39 G. F. Fedorin and V. P. Georgievskii, *J. Appl. Spectrosc.*, 1974, **20**, 122.
40 P-S Song, M. L. Harter, T. A. Moore and W. E. Herdon, *Photochem. Photobiol.*, 1971, **14**, 521.
41 S. Rajadurai and P. K. Das, *Can. J. Chem.*, 1987, **65**, 2277.
42 J. W. Hanifin and E. Cohen, *J. Am. Chem. Soc.*, 1969, **91**, 4494.
43 R. W. Tuveson, R. A. Larson and J. Kagan, *J. Bacteriol*, 1980, **179**, 4675.
44 K. R. Downum, W. E. Hancock and G. H. N. Towers, *Photochem. Photobiol.*, 1982, **36**, 577.
45 R. W. Tuveson, G. Wong and R. S. Becker, *Photochem. Photobiol.*, 1992, **56**, 34.

Paper 2/05997E; *Received* 10*th November*, 1992